RSC Advances

PAPER

View Article Online
View Journal | View Issue

Cite this: *RSC Adv.*, 2017, **7**, 19330

Use of CuO encapsulated in mesoporous silica SBA-15 as a recycled catalyst for allylic C–H bond oxidation of cyclic olefins at room temperature†

Saadi Samadi,*[ab] Akram Ashouri[a] and Mehdi Ghambarian[c]

Received 13th March 2017
Accepted 17th March 2017

DOI: 10.1039/c7ra02995k

rsc.li/rsc-advances

CuO nanoparticles were deposited on SBA-15 in three routes. These were metal loading on SBA-15 and calcination at 550 °C (Cu–SBA-15), metal loading on 3-aminopropyl-trimethoxysilane grafted SBA-15 and calcination at 550 °C (Cu–N–SBA-15), and metal loading on 3-aminopropyl-trimethoxysilane grafted SBA-15 and reduction by $NaBH_4$ then calcination at 550 °C (Cu–B–N–SBA-15). These catalysts were characterized through powder X-ray diffraction (XRD), BET nitrogen adsorption–desorption methods, energy dispersive X-ray (EDX), atomic absorption spectroscopy (AAS), elemental mapping, scanning electron microscopy (SEM), and Fourier transform infrared (FT-IR) spectroscopy. The result of the heterogeneous catalysts being applied in the monometallic direct catalytic esterification of sp^3 C–H bonds in cyclic olefins for the first time is reported, using *tert*-butyl 4-nitrobenzoperoxoate at room temperature. Allylic esters were obtained as the product of the C–H bond oxidation reaction in moderate to good yields (up to 99%) within reasonable reaction times. Also, the recovered catalyst (Cu–B–N–SBA-15) is applicable in the oxidation reaction for four times with little loss in reactivity and yield.

1. Introduction

The direct functionalization of sp^3 C–H bonds is one of the most important reactions in organic synthesis.[1–4] Oxidation reaction of these bonds at the allylic position of cycloolefins (Kharash–Sosnovsky reaction) can be used as one of the most straightforward synthetic routes for the preparation of highly functionalized olefins such as allylic esters and allylic alcohols that are important intermediates in the synthesis of leukotriene B_4 (ref. 5) chrysanthemic acid,[6] brevetoxin[7] and amyrin.[8] The nature of the metal salt, perester oxidant, and reaction conditions including solvent and temperature are affected this reaction remarkably.[9–17]

Allylic C–H bond oxidation have been studied by homogeneous catalysts such as selenium,[18–24] selenium dioxide,[18–21,23] diselenides[24] and pentafluorobenzeneselenic acid[18–24] with different metals such as Hg(II),[25–30] Pd(II),[31–37] Pb(IV),[25] Cr(VI),[25,38,39] Co(III),[40,41] Co(II),[42–44] Mn(III),[41,45,46] Ce(IV),[41] Fe(II),[47] Rh(II),[48] Rh(I),[49,50] Cu[5–13] and a variety of ligands. However, copper-catalysis – due to its low cost – is the most popular in this field, although their large industrial scale usage is limited.

On the other side, supported nanometals are one of the most important categories of heterogeneous catalysts with broad applications in the industry. Some materials, such as SBA-15, MCM-41 and zeolite were applied for the preparation of metal nanoparticles.

Among them, SBA-15 has some advantages such as hexagonally arrayed channels and narrow pore size distribution so that it has attracted great attention.[51–53] Immobilization of metal NPs within a silica scaffold prevents agglomeration and surface fouling, and aids in NP recovery and recycling.[54–57]

In our previous work, we reported the effect of some additives such activated silica gel, mesoporous MCM-41, SBA-15 silica, nanocrystalline MgO, CuO and TiO_2 on this reaction and SBA-15 was shown better results than others.[58–61] The strong effect of these additives encouraged us to prepare and characterize CuO encapsulated in mesoporous silica SBA-15 with various Cu loadings in the range of 1–12 wt% by an impregnation method in three routes, which was applied in allylic C–H bond oxidation of cyclic olefins.[1–13]

2. Experimental

2.1. General remarks

All reagents and starting materials were purchased from Aldrich, Merck, Fluka and Sigma. Cycloolefins were distilled

[a]*Laboratory of Asymmetric Synthesis, Department of Chemistry, Faculty of Science, University of Kurdistan, Zip Code 66177-15175, Sanandaj, Iran. E-mail: s.samadi@uok.ac.ir*

[b]*Research Centre of Nanotechnology, University of Kurdistan, P.O. Box 416, Sanandaj, Iran*

[c]*Gas Conversion Department, Faculty of Petrochemicals, Iran Polymer and Petrochemical Institute, P.O. Box 14975-112, Tehran, Iran*

† Electronic supplementary information (ESI) available: Supplementary data (included IR, ^1H and ^{13}C spectra of compounds **1–5** and the procedure of synthesis **1**, IR, SEM, EDX, X-ray scattering and elemental mapping for prepared catalysts and the typical procedure for the synthesis of SBA-15, NH_2–SBA-15). See DOI: 10.1039/c7ra02995k

from calcium hydride before use. All solvents for the reactions were also dried and distilled immediately before use. Melting points were measured on an Electrothermal 9100 apparatus and are uncorrected. Fourier transform infrared (FT-IR) spectrum was recorded on a Bruker Vector 22 spectrometer using pressed KBr pellets. X-ray diffraction patterns were obtained on a Simens D500 diffractometer with Cu Kα radiation. The SEM image and EDX patterns were taken using VEGA\\-TESCAN. The surface area was calculated by the BET method in Quantachrome Instruments.

2.2. The preparation of heterogeneous catalysts

The preparation of Cu–B–N–SBA-15 was drown in Scheme 1.

2.2.1. Typical procedure for Cu–SBA-15. A round-bottomed flask (50 mL) equipped with a stirrer bar was charged with 2 g of SBA-15 (ref. 62) and ethanol (20 mL). Then $Cu(NO_3)_2$ was added to the reaction mixture and stirred for 10 h at room temperature. The resultant material was collected by filtration and washed thoroughly with C_2H_5OH, dried at 100 °C and calcined at 550 °C for 5 h (S2–S4, S8 and S9 in ESI† and Fig. 1–3).[51–53]

2.2.2. Typical procedure for Cu–N–SBA-15 (ref. 51). The procedure for preparation of this catalyst was same as 2.2.1. but NH_2–SBA-15 (ref. 63) was used instead of SBA-15 (S5–S7, S10–S13 in ESI† and Fig. 1–3).

2.2.3. Typical procedure for Cu–B–N–SBA-15. To produce this catalyst, the same procedure was used as 2.2.2. with this difference that before calcination step, the modified mesoporous stirred with 10 mL of 0.1 M $NaBH_4$ ethanol solution at room temperature for 2 hours.[51] (Fig. 1–3).

2.3. Allylic C–H bond oxidation of cyclic olefins

Allylic oxidation of cycloolefins was drown in Scheme 2.

2.3.1. General procedure for allylic C–H bond oxidation of cycloolefins by using *tert*-butyl 4-nitrobenzoperoxoate. The heterogonous catalyst was preheated under vacuum at 80 °C for 2 h. To a round bottom flask (25 mL), 40 mg of dried heterogonous catalyst, cycloolefin (5 mmol) and acetonitrile (4 mL) were added and stirred for 30 minute at room temperature then *tert*-butyl *p*-nitrobenzoperoxoate **1** (0.203 g, 0.85 mmol)[58] was added slowly. The mixture was stirred until TLC showed the complete consumption of the perester.

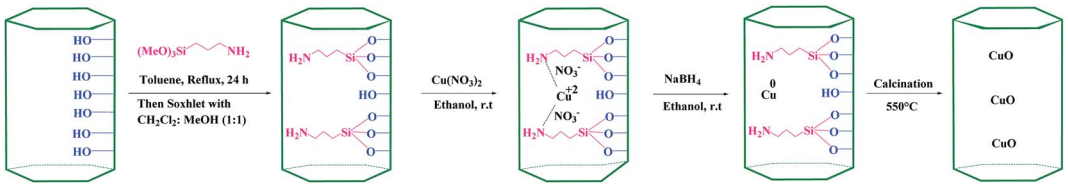

Scheme 1 Synthesis of Cu–B–N–SBA-15.

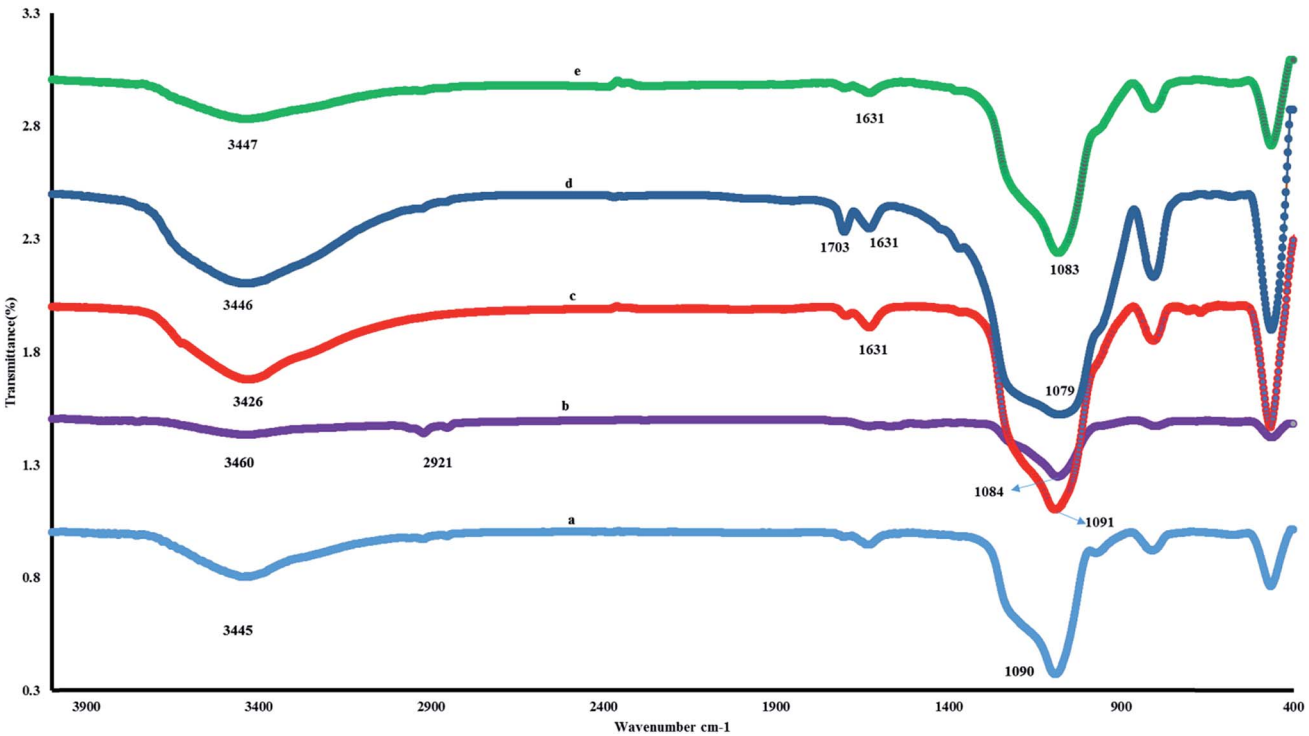

Fig. 1 FT-IR spectra of SBA-15 (a), NH_2–SBA-15 (b), Cu–SBA-15 (c), Cu–N–SBA-15 (d), Cu–B–N–SBA-15 (e).

When the reaction was completed, the heterogonous catalyst was isolated by filtration, and then thoroughly washed three times with methylene chloride and air-dried. After filtration, the methylene chloride phase was washed with saturated aqueous NH_4Cl (10 mL) after that saturated aqueous $NaHCO_3$ (10 mL) and dried over $MgSO_4$. The solvent was evaporated under vacuum, and the product purified with column chromatography (ethyl acetate/*n*-hexane 2–10%) to afford white solid up to 99% yield (S14–24 in the ESI†).[58–61]

*Cyclopent-2-en-1-yl 4-nitrobenzoate (**2**).* Mp: 76–79 °C (lit. 77–79 °C (ref. 58)); R_f = 0.57 (90 : 10, *n*-hexane : EtOAc); ^{1}H NMR (300 MHz, $CDCl_3$): δ_H (ppm) = 1.94–2.00 (1H, m), 2.41–2.50 (2H, m), 2.59–2.67 (1H, m), 6.05 (2H, m), 6.33 (1H, m), 8.25 (d, 2H, J = 8.7 Hz), 8.29 (d, 2H, J = 8.7 Hz); ^{13}C NMR (75 MHz, $CDCl_3$): δ_C (ppm) = 29.2, 31.3, 81.7, 123.5, 128.4, 131.1, 136.6, 139.1, 150.6, 165.2.

*Cyclohex-2-en-1-yl 4-nitrobenzoate (**3**).* Mp: 68–70 °C (lit. 68–71 °C (ref. 58)); R_f = 0.64 (*n*-hexane : EtOAc; 90 : 10), ^{1}H NMR (300 MHz, $CDCl_3$): δ_H (ppm) = 1.77–2.14 (6H, m), 5.61 (1H, m), 5.87 (1H, d, J = 10.1 Hz), 6.10 (1H, d, J = 10.1 Hz), 8.18–8.28 (4H, m); ^{13}C NMR (75 MHz, $CDCl_3$): δ_C (ppm) = 18.8, 25.0, 28.2, 69.8, 123.4, 125.0, 130.7, 133.6, 136.2, 150.4, 164.3.

Table 1 BET surface area of SBA-15, NH_2–SBA-15, Cu–SBA-15, Cu–N–SBA-15, Cu–B–N–SBA-15

Entry	Sample	BET surface area (m^2 g^{-1})
1	SBA-15	912
2	Cu–SBA-15	438
3	NH_2–SBA-15	544
4	Cu–N–SBA-15	305
5	Cu–B–N–SBA-15	293

*Cyclooct-2-en-1-yl 4-nitrobenzoate (**4**).* Mp: 72–73 °C (lit. 71–74 °C (ref. 58)); R_f = 0.67 (*n*-hexane : EtOAc; 90 : 10); ^{1}H NMR (300 MHz, $CDCl_3$): δ_H (ppm) = 1.51–1.76 (7H, m), 2.11–2.40 (3H, m), 5.56–5.59 (1H, m), 5.77–5.85 (1H, m), 5.90–5.94 (1H, m), 8.28–8.36 (4H, m); ^{13}C NMR (75 MHz, $CDCl_3$): δ_C (ppm) = 22.8, 24.9, 25.2, 30.8, 35.7, 73.8, 124.1, 130.4, 131.1, 133.0, 149.7, 165.8.

*Cycloocta-2,6-dien-1-yl 4-nitrobenzoate (**5**).* Mp: 72–75 °C (lit. 74–76 °C (ref. 58)); R_f = 0.62 (*n*-hexane : EtOAc; 90 : 10); ^{1}H NMR (300 MHz, $CDCl_3$): δ_H (ppm) = 2.21–2.41 (2H, m), 2.54–2.68 (2H, m), 2.85–2.95 (2H, m), 5.57–5.84 (4H, m), 6.17–6.26 (1H, m),

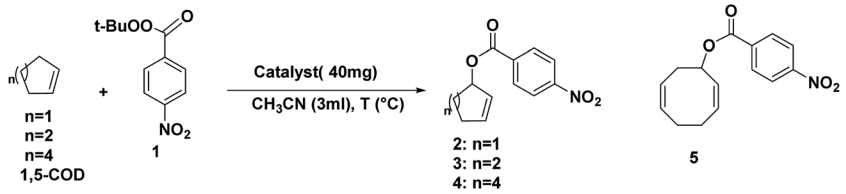

Scheme 2 Allylic C–H bond oxidation of cyclic olefins in the presence of heterogeneous catalyst.

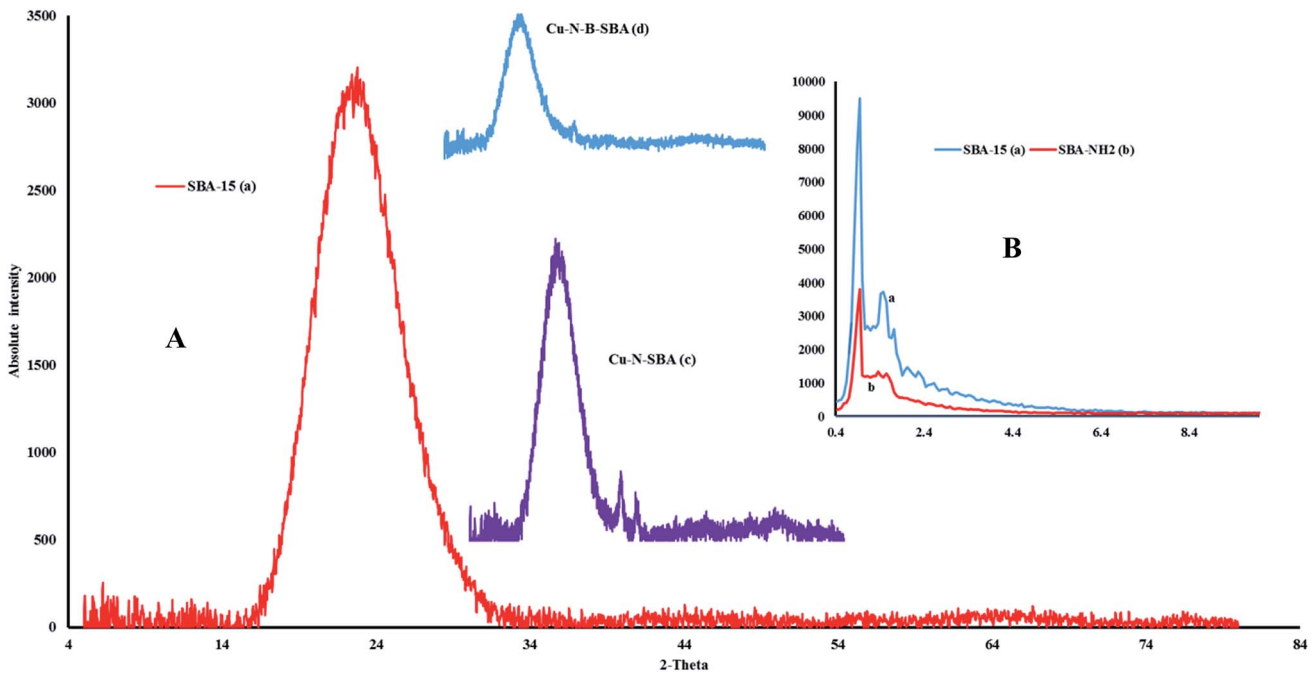

Fig. 2 (A) Wide angle X-ray diffraction patterns of SBA-15, Cu–N–SBA-15, Cu–B–N–SBA-15. (B) Low angle X-ray diffraction patterns of SBA-15, NH_2–SBA-15.

8.23 (2H, d, J = 8.5 Hz), 8.30 (2H, d, J = 8.4 Hz); ^{13}C NMR (75 MHz, $CDCl_3$): δ_C (ppm) = 27.6, 28.1, 28.5, 74.6, 124.3, 125.2, 128.3, 129.4, 131.3, 132.5, 133.4, 150.2, 167.5.

3. Results and discussions

3.1. Characterization of heterogeneous catalyst

The catalyst was characterized by XRD, EDX, BET, SEM, AAS and FT-IR.

3.1.1. Spectroscopic characterization. SBA-15, NH_2–SBA-15, Cu–SBA-15, Cu–N–SBA-15, and Cu–B–N–SBA-15 were analyzed by FT-IR in the 400–4000 cm^{-1} region (Fig. 1). The wide bands at 1079–1250 cm^{-1} were remarked as Si–O–Si bands of the condensed silica network. The peak 803–806 cm^{-1} can be assigned to the symmetric stretching vibration of Si–O. In the case of Cu–SBA-15, the characteristic bands were appeared at 804 and 1087 cm^{-1}.

The NH_2–SBA-15 (b spectrum) was considered by peaks at 1392 and 1553 cm^{-1} which confirmed successfully immobilization of the amine functional group onto SBA-15. Characterized bands in Cu–N–SBA-15 at 805, 1079, 1631 and 1703 cm^{-1} and regarded bonds 806, 1083 and 1631 cm^{-1} for Cu–B–N–SBA-15 clearly demonstrated that the mesoporous structure of SBA-15 preserved after modification (Fig. 1).

Low angle X-ray diffraction patterns of SBA-15 showed a peak at 2θ = 0.94°, corresponding to the (100) reflection, and two weak reflections at about 1.47 and 1.8°. Comparison the X-ray patterns of NH_2–SBA-15 with SBA-15 shows that the hexagonal pore structures of SBA-15 has been retained after the immobilization of (3-aminopropyl)trimethoxysilane in SBA-15 (Fig. 2B).

To prove the existence of copper on the surface of calcined catalysts, the wide angle X-ray diffraction pattern of SBA-15 and Cu-containing samples (SBA-15–N–Cu and SBA-15–N–B–Cu) were investigated.[51]

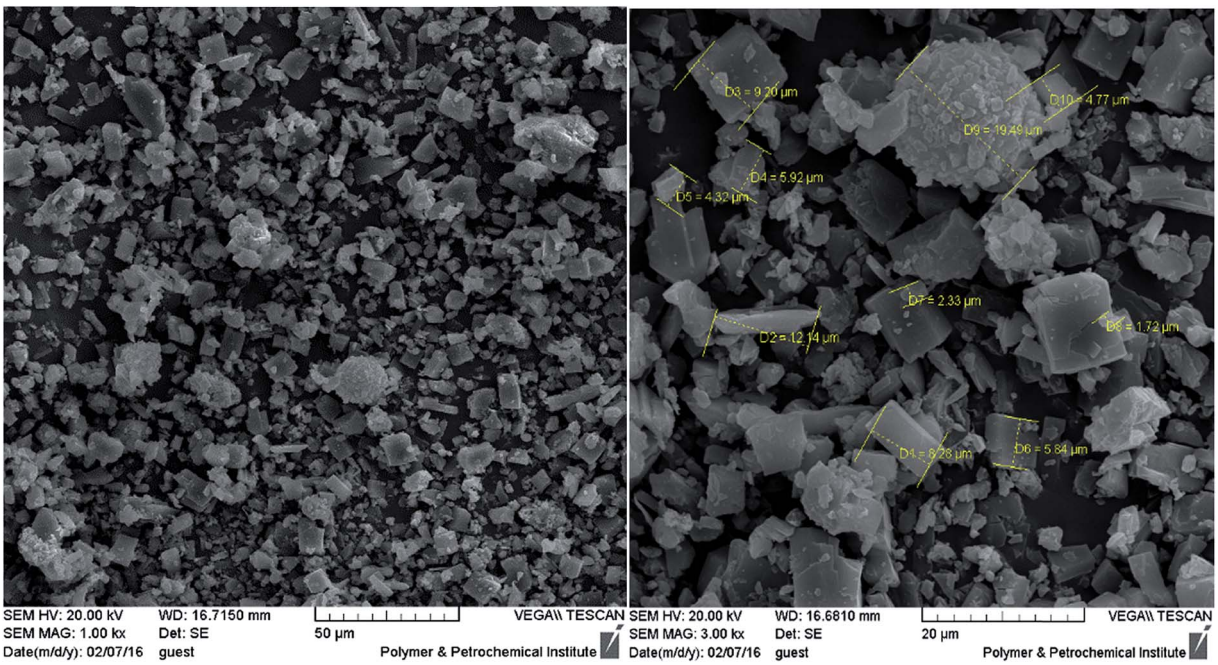

Fig. 3 Scanning electron micrographs of Cu–B–N–SBA-15.

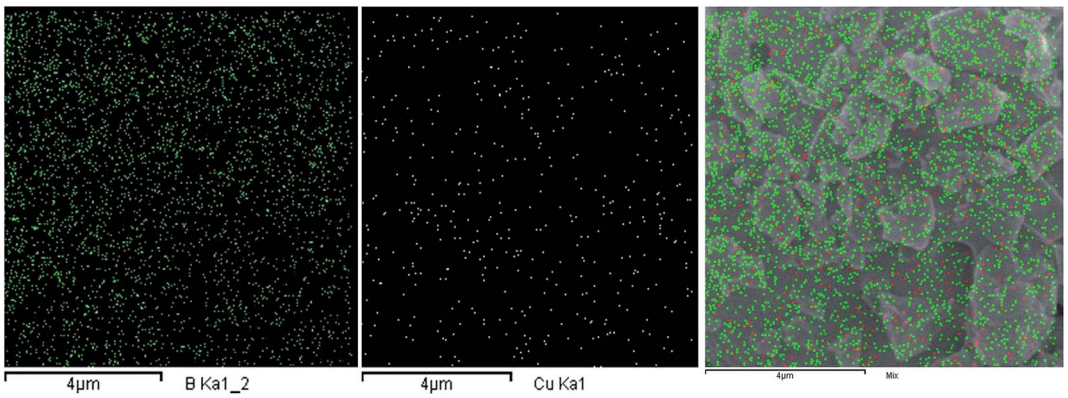

Fig. 4 Elemental mapping of the Cu–B–N–SBA-15 catalysts.

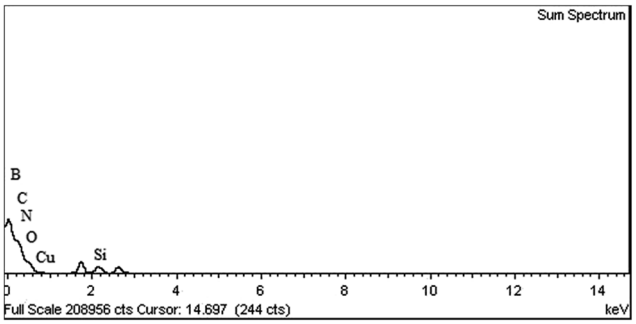

Fig. 5 EDX spectrum of the Cu–B–N–SBA-15 catalysts.

Table 2 Effect of homogeneous and heterogeneous catalyst on reaction at different temperatures in acetonitrile[a,b]

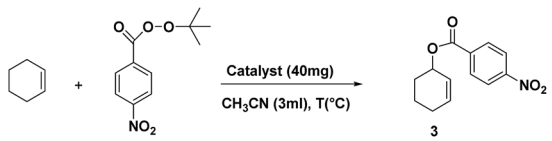

Entry	Catalyst	Temperature (°C)	Time (h)	Yield (%)
1	CuOAc	25	120	62
2	$Cu(NO_3)_2$	25	110	65
3	$CuSO_4$	25	>200	55
4	CuO	25	>200	45
5	Cu_2O	25	<100	54
6	Cu–SBA-15	25	37	80
7	Cu–N–SBA-15	25	34	87
8	Cu–B–N–SBA-15	25	25	99
9	Cu–SBA-15	40	30	84
10	Cu–N–SBA-15	40	28	90
11	Cu–B–N–SBA-15	40	30	95
12	Cu–SBA-15	Reflux	32	85
13	Cu–N–SBA-15	Reflux	27	93
14	Cu–B–N–SBA-15	Reflux	27	95

[a] Reaction conditions: **1** (0.2 mmol), cyclohexene (5 mmol), catalyst (40 mg), in 3 mL CH_3CN stirred. [b] Isolated yield.

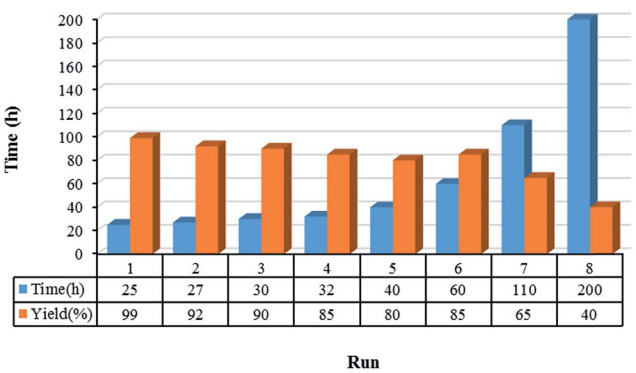

Fig. 6 Correlation between recyclability of Cu–B–N–SBA-15 with time and yield%.

Table 3 Effect of solvent on reaction at different temperatures[a,b]

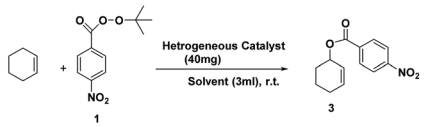

Entry	Catalyst	Solvent	Time (h)	Yield (%)
1	Cu–SBA-15	CH_3CN	37	80
2	Cu–N–SBA-15	CH_3CN	34	87
3	Cu–B–N–SBA-15	CH_3CN	25	99
4	Cu–SBA-15	Acetone	25	75
5	Cu–N–SBA-15	Acetone	40	77
6	Cu–B–N–SBA-15	Acetone	20	82
7	Cu–SBA-15	CH_2Cl_2	86	25
8	Cu–N–SBA-15	CH_2Cl_2	62	28
9	Cu–B–N–SBA-15	CH_2Cl_2	70	22
10	Cu–SBA-15	DMF	70	35
11	Cu–N–SBA-15	DMF	50	40
12	Cu–B–N–SBA-15	DMF	52	45

[a] Reaction conditions: **1** (0.2 mmol), cyclohexene (5 mmol), heterogeneous catalyst (40 mg), in 3 mL solvents stirred at r.t. [b] Isolated yield.

As Fig. 2A shows, the reflection of Cu–N–SBA-15 at $2\theta = 23.5°$ and for Cu–B–N–SBA-15 at $2\theta = 23.7°$ with decreased intensity was remained after impregnation in compare with SBA-15 at $2\theta = 24.2°$.

The reflexes assigned for CuO in Cu–N–SBA-15 at $2\theta = 35.4°$, 38.3° and 47.4°, for Cu–B–N–SBA-15, CuO at $2\theta = 35.4°$, 38.6° and Cu_2O at $2\theta = 37.3°$.[51] Also wide angle X-ray diffraction patterns powder X-ray diffraction data demonstrated that the hexagonal structure of SBA-15 has been preserved during the process of catalyst preparation.

Table 4 Effects of copper loading in Cu–B–N–SBA-15 on oxidation reaction[a,b]

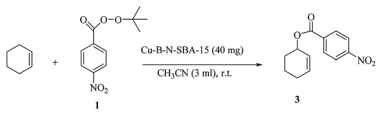

Entry	Cu	Time (h)	Yield (%)
1	1%	150	35
2	2%	120	40
3	3%	90	46
4	4%	60	57
5	5%	48	64
6	6%	40	70
7	7%	36	80
8	8%	30	87
9	9%	25	99
10	10%	46	67
11	11%	59	55
12	12%	75	40

[a] Reaction conditions: **1** (0.2 mmol), cyclohexene (5 mmol), Cu–B–N–SBA-15 (40 mg), in 3 mL CH_3CN stirred at r.t. [b] Isolated yield.

BET surface area of SBA-15, NH_2–SBA-15, Cu–N–SBA-15 and Cu–B–N–SBA-15 are presented in Table 1. A significant decrease in the amount of nitrogen adsorption was observed with incorporation of copper in SBA-15, which means that the specific surface area of Cu–SBA-15 decreases in compared with pure siliceous SBA-15. These amounts of 912 $m^2\ g^{-1}$ for SBA-15 were decreased to 305 $m^2\ g^{-1}$ for Cu–N–SBA-15 and 293 $m^2\ g^{-1}$ for Cu–B–N–SBA-15.

Morphological changes were investigated by SEM for SBA-15, NH_2–SBA-15, Cu–SBA-15, Cu–N–SBA-15 (S4, S7, S10 and S13 in the ESI†) and Cu–B–N–SBA-15 (Fig. 3).

Elemental composition of heterogeneous catalysts and the dispersity of metal-oxide nanoparticles in the SBA-15 are further clarified by elemental mapping. This technique illustrated the homogeneous dispersion of metallic CuO over the mesoporous support (Fig. 4, S14 and S15 in the ESI†).

EDX was used to qualitatively distinguish the present elements (Fig. 5, S5, S8 and S11 in the ESI†). The amounts of copper in Cu–SBA-15, Cu–N–SBA-15, and Cu–B–N–SBA-15 were determined by using atomic absorption spectroscopy 6.54, 8.83 and 8.86 wt% respectively.

Table 5 Effects of catalyst loading of Cu–B–N–SBA-15 (Cu content 9%) on reaction[a,b]

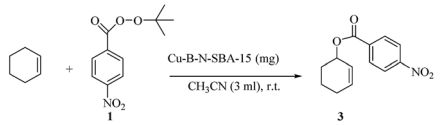

Entry	Catalyst (mg)	Time (h)	Yield (%)
1	40	25	99
2	20	55	70
3	60	43	80
3	10	90	50

[a] Reaction conditions: **1** (0.2 mmol), cyclohexene (5 mmol), Cu–B–N–SBA-15 (mg), in 3 mL CH_3CN stirred at r.t. [b] Isolated yield.

3.2. Catalytic effects in allylic C–H bond oxidation of cyclic olefins

3.2.1. Optimization of the model reaction. The catalytic activity of these catalysts was investigated in the copper-catalyzed direct esterification of inert C–H bonds in cycloolefins. The optimization of the reaction conditions were carried out by using cyclohexene as the substrate and *tert*-butyl *p*-nitro perbenzoate **1** as an oxidant (S17–19 in the ESI†)[61] in the presence of various homogeneous and heterogeneous catalyst in acetonitrile at different temperature (Table 2).

When the reaction was catalyzed by different Cu salts as homogenous catalyst, a low yielding reaction was observed (entries 1–5). Whereas by using heterogeneous catalysts which Cu is encapsulated in SBA-15, reaction yields and rates were considerably increased (entries 6–14 in Table 2).

The best result was achieved with 40 mg of Cu–B–N–SBA-15, which afforded 2-cyclohexenyl-*p*-nitrobenzoate **3** (S14 and S15 in the ESI†) as product with 99% yield in 25 h at room temperature (entry 9, Table 2). These results support the high activity of Cu catalysts in the cyclohexene oxidation.

According to spectroscopic results, Cu–B–N–SBA-15 catalyst has CuO and Cu_2O. However, the rate of this reaction is increased by this catalyst due to the existence of Cu_2O. It worth mentioning that, the active copper species involving in allylic oxidation reactions is copper(I).[51,58–61] The elemental mapping of this catalyst proves the existence of boron element which is able act as Lewis acid in allylic C–H bond oxidation of cyclic olefins (Fig. 5 and 6).

The effect of various solvents were investigated. The yield was increased gradually with increasing polarity of solvents. It was observed that acetonitrile is the best solvent for this reaction (Table 3, entry 3).

The effects of copper and catalyst loading were also evaluated. The results which described in Tables 4 and 5 showed that the time and yield of reaction were affected by the amount of copper doping and the amount of catalyst. The best results were achieved when approximately 9 wt% loading of copper and 40 mg of catalyst per 5 mmol of substrate (cyclohexene) were

Table 6 Synthesis of allylic esters **2**, **4**, **5** by allylic oxidation of various cycloolefins over heterogeneous catalyst[a,b]

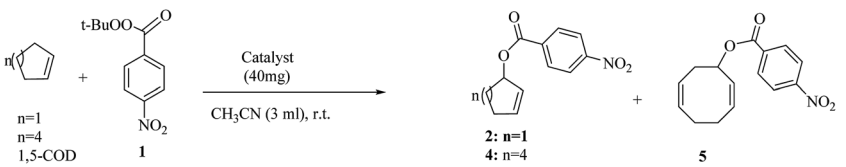

		2		4		5	
Entry	Catalyst	Time (h)	Yield (%)	Time (h)	Yield (%)	Time (h)	Yield (%)
1	CuO	>250	22	>200	15	>150	28
2	Cu–SBA-15	80	54	100	60	42	75
3	Cu–N–SBA-15	64	65	75	80	35	80
4	Cu–B–N–SBA-15	50	80	50	90	22	85

[a] Reaction conditions: **1** (0.2 mmol), cycloolefins (5 mmol), catalyst (40 mg), in 3 mL MeCN stirred at r.t. [b] Isolated yield.

used (Table 4, entry 9 and Table 5, entry 1). Lowering the copper loading to less than 4 wt% and increasing of this amount to 9 wt% led to sharp decrease in the desired results. The copper content was analyzed by AAS.

Various allylic esters from different cycloolefins (S20–28 in the ESI†) were prepared under the optimized conditions, and the results are shown in Table 6. The achieved results in the presence of Cu–B–N–SBA-15 were better than others.

3.2.2. Recycling of the catalyst. The recovery and recyclability of the Cu–B–N–SBA-15 for allylic C–H bond oxidation of cyclohexene was evaluated. As shown in Fig. 6, the catalyst was reused for subsequent runs, up to four times with little loss in activity.

The mesoporous structure preservation of Cu–B–N–SBA-15 after eighth times recycling, was confirmed by XRD, SEM and IR results. After completion of the reaction, the mesoporous Cu–B–N–SBA-15 was recovered by simple filtration, washed with ethanol and distilled water, dried at 70 °C for 4 h under vacuum and reused in the subsequent run.

4. Conclusions

In conclusion, CuO encapsulated in mesoporous silica SBA-15 as monometallic catalysts has been synthesized through the reaction of SBA-15 or aminopropyl modified SBA-15 with $Cu(NO_3)_2$ under different conditions. The catalytic potential of these heterogeneous catalysts was applied for the copper-catalyzed allylic oxidation of cycloolefins *via* sp^3 C–H bond activation. Allylic esters were prepared in good yields, reasonably short period of time and high selectivity in acetonitrile in the presence of 40 mg of Cu–B–N–SBA-15 with 9 wt% loading of copper. For cyclohexene in comparison with other cycloolefins, the best result in term of yield (99%) and rate of reaction (25 h) was obtained.

Mild conditions of this reaction in combination with recyclability of the catalyst, make the presented work a desire approach to produce functionalized olefins in compared to the most of reports.

Acknowledgements

We are grateful to the University of Kurdistan Research Councils for the support of this work.

References

1 C. Zheng and S. L. You, *RSC Adv.*, 2014, **4**, 6173–6214.
2 F. L. Zhang, K. Hong, T. J. Li, H. Park and J. Q. Yu, *Science*, 2016, **351**, 252–256.
3 J. D. Cuthbertson and D. W. MacMillan, *Nature*, 2015, **519**, 74–77.
4 J. F. Hartwig and M. A. Larsen, *ACS Cent. Sci.*, 2016, **2**, 281–292.
5 R. Hayes and T. W. Wallace, *Tetrahedron Lett.*, 1990, **31**, 3355–3356.
6 J. Finici and J. d'Angelo, *Tetrahedron Lett.*, 1976, **17**, 2441–2459.
7 E. Alvarez, M. T. Diaz, R. Perez, J. L. Ravelo, A. Regueiro, J. A. Vera, D. Zurita and J. D. Martin, *J. Org. Chem.*, 1994, **59**, 2848–2876.
8 E. J. Corey and J. Lee, *J. Am. Chem. Soc.*, 1993, **115**, 8873–8874.
9 D. J. Rawlinson and G. Sosnovsky, *Synthesis*, 1972, 1–28.
10 J. C. Frison, J. Legros and C. Bolm, Copper and Palladium Catalyzed Allylic Acyloxylations, in *Handbook of CH Transformations*, ed. G. Dyker, Wiley-VCH, Weinheim, 2005.
11 M. S. Kharasch, G. Sosnovsky and N. C. Yang, *J. Am. Chem. Soc.*, 1958, **80**, 756.
12 M. S. Kharash and A. Fono, *J. Org. Chem.*, 1958, **23**, 324.
13 M. S. Kharash and A. Fono, *J. Org. Chem.*, 1958, **23**, 325.
14 M. S. Kharasch, G. Sosnovsky and N. C. Yang, *J. Am. Chem. Soc.*, 1959, **81**, 5819–5824.
15 A. L. Beckwith and A. A. Zavitsas, *J. Am. Chem. Soc.*, 1986, **108**, 8230–8234.
16 J. K. Kochi and A. Bemis, *Tetrahedron*, 1968, **24**, 5099–5113.
17 C. Walling and A. A. Zavitsas, *J. Am. Chem. Soc.*, 1963, **85**, 2084.
18 H. Rapoport and U. T. Bhalerao, *J. Am. Chem. Soc.*, 1971, **93**, 4835–4840.
19 M. J. Francis, P. K. Grant, K. S. Low and R. T. Weavers, *Tetrahedron*, 1976, **32**, 95–101.
20 M. A. Umbreit and K. B. Sharpless, *J. Am. Chem. Soc.*, 1977, **99**, 5526–5528.
21 W. Woggon, F. Ruther and H. Egli, *J. Chem. Soc., Chem. Commun.*, 1980, 706–708.
22 M. lwaoka and S. Tomoda, *J. Chem. Soc., Chem. Commun.*, 1992, 1165–1166.
23 K. Shibuya, *Synth. Commun.*, 1994, **24**, 2923–2941.
24 D. H. R. Barton and T. Wang, *Tetrahedron Lett.*, 1994, **35**, 5149–5152.
25 K. B. Wiberg and S. D. Nielsen, *J. Org. Chem.*, 1964, **29**, 3353–3361.
26 Z. Rappoport, P. D. Sleezer, S. Winstein and W. G. Young, *Tetrahedron Lett.*, 1965, **26**, 3719–3721.
27 Z. Rappoport, P. D. Sleezer, S. Winstein and W. G. Young, *J. Am. Chem. Soc.*, 1972, **94**, 2320–2322.
28 K. B. Sharpless and R. F. Lauer, *J. Am. Chem. Soc.*, 1972, **94**, 7154–7155.
29 D. Arigoni, A. Vasella, K. B. Sharpless and H. P. Jensen, *J. Am. Chem. Soc.*, 1973, **95**, 7917–7919.
30 D. A. Singleton and C. Hang, *J. Org. Chem.*, 2000, **65**, 7554–7560.
31 K. William, S. Winstein, W. G. Young and Z. Rappoport, *J. Am. Chem. Soc.*, 1966, **88**, 2054–2055.
32 S. Uemura, S. Fukuzawa, A. Toshimitsu and M. Okano, *Tetrahedron Lett.*, 1982, **23**, 87–90.
33 J. E. McMurry and P. Kocovsky, *Tetrahedron Lett.*, 1984, **25**, 4187–4190.
34 C. Jia, P. Müller and H. Mimoun, *J. Mol. Catal. A: Chem.*, 1995, **101**, 127–133.
35 N. Y. Kozitsyna, M. N. Vargaftik and I. I. Moiseev, *J. Organomet. Chem.*, 2000, **593–594**, 274–291.
36 A. K. El-Qisiari, H. A. Qaseer and P. M. Henry, *Tetrahedron Lett.*, 2002, **43**, 4229–4231.

37 I. l. Moiseev and M. N. Vargaftik, *Coord. Chem. Rev.*, 2004, **248**, 2381–2391.
38 W. G. Dauben, M. Lorber and D. S. Fullerton, *J. Org. Chem.*, 1969, **34**, 3587–3592.
39 P. Müller and T. T. Khoi, *Tetrahedron Lett.*, 1977, **18**, 1939–1942.
40 M. Hirano, K. Nakamura and T. Morimoto, *J. Chem. Soc., Perkin Trans. 2*, 1981, 817–820.
41 T. Morimoto, T. Machida, M. Hirano and X. Zhung, *J. Chem. Soc., Perkin Trans. 2*, 1981, 909–913.
42 H. Alper and M. Harustiak, *J. Mol. Catal.*, 1993, **84**, 87–92.
43 T. Punniyamurthy and J. Iqbal, *Tetrahedron Lett.*, 1994, **35**, 4003–4006.
44 H. Alper and M. Harustiak, *J. Mol. Catal.*, 1993, **84**, 87–92.
45 J. R. Gilmore and J. M. Mellor, *J. Chem. Soc. C*, 1971, 2355–2357.
46 F. J. McQuillin and M. Wood, *J. Chem. Res.*, 1977, 61.
47 F. Minisci and R. Galli, *Tetrahedron Lett.*, 1963, 357–360.
48 S. Uemura and S. R. Patil, *Chem. Lett.*, 1982, 1743–1746.
49 J. E. Baldwin and J. C. Swallow, *Angew. Chem., Int. Ed. Engl.*, 1969, **8**, 601–602.
50 A. Morvillo and M. Bressan, *J. Mol. Catal.*, 1986, **37**, 63–74.
51 J. Czaplinska, I. Sobczak and M. Ziolek, *J. Phys. Chem. C*, 2014, **118**, 12796–12810.
52 G. Saidulu, N. Anand, K. S. R. Rao, A. Burri, S. E. Park and D. R. Burri, *Catal. Lett.*, 2011, **141**, 1865–1871.
53 A. Narani, R. K. Marella, P. Ramudu, K. S. R. Rao and D. R. Burri, *RSC Adv.*, 2014, **4**, 3774–3781.
54 T. Asefa, A. Anan, C. T. Duncan and Y. Xie *Invited Chapter of a Book "Non Magnetic Bi-Metallic and Metal Oxide Nanomaterials for Life Sciences"*, ed. C. S. S. R. Kumar, Wiley-VCH, 2009.
55 T. Asefa, C. T. Duncan and K. K. Sharma, *Analyst*, 2009, **134**, 1980–1990.
56 Y. Hao, Y. Chong, S. Li and H. Yang, *J. Phys. Chem. C*, 2012, **116**, 6512–6519.
57 H. Yang, Z. Ma, T. Zhou, W. Zhang, J. Chao and Y. Qin, *ChemCatChem*, 2013, **5**, 2278–2287.
58 S. Samadi, K. Jadidi and B. Notash, *Tetrahedron: Asymmetry*, 2013, **24**, 269–277.
59 S. Samadi, S. Nazari, H. Arvinnezhad, K. Jadidi and B. Notash, *Tetrahedron*, 2013, **69**, 6679–6686.
60 L. Faraji, S. Samadi, K. Jadidi and B. Notash, *Bull. Korean Chem. Soc.*, 2014, **35**, 1989–1995.
61 S. Samadi, K. Jadidi, B. Khanmohammadi and N. Tavakoli, *J. Catal.*, 2016, **340**, 344–353.
62 D. Zhao, J. Feng, Q. Huo, N. Malosh, G. H. Fredrickson, B. F. Chmelka and G. D. Stucky, *Science*, 1998, **279**, 548–552.
63 X. Zhang, E. Sau Man Lai, R. Martin-Aranda and K. L. Yeung, *Appl. Catal., A*, 2004, **261**, 109–118.